

ASSESSMENT OF SURFACE COAL MINING IMPACTS USING LANDSAT TIME SERIES DATA

V. Saini^{1*}, Manoj K. Arora² and R. P. Gupta¹

¹Indian Institute of Technology Roorkee, Roorkee, Uttarakhand-247667, India,
Email: *varinder126@gmail.com; rpgupta.iitr@gmail.com

²PEC University of Technology, Chandigarh-160012, India,
Email: manoj.arora@gmail.com

KEYWORDS: Environmental impacts; NDVI; Tasseled Cap Transformation; Surface temperature; Jharia coalfield

ABSTRACT

Mining is an integral part of the development of many countries in the world and is associated with adverse environmental impacts. It, therefore, becomes pertinent to optimize and minimize these impacts by adopting proper mining techniques. For this, it is necessary to have quickly accessible, cost-effective and periodical information regarding the area. Satellite remote sensing is able to provide such data. The Jharia coalfield (JCF) in the state of Jharkhand is the only coking coal mine in India. It is also infamous for its surface and subsurface coal fires which have been burning now for more than a century. Surface mining is the dominant driver of land use/land cover change here. Large scale deforestation has affected ecosystem services such as aesthetics, biodiversity and availability of clean air. Coal fires have caused not only severe environmental pollution by toxic exhaust gases but also have left many landscapes devoid of vegetation and uninhabitable. To study the impact of surface coal mining activities in a part of JCF, a multi-temporal analysis of Landsat (TM and OLI/TIRS) data has been undertaken for the years between 2006 and 2016. Two indices namely Normalized Difference Vegetation Index (NDVI) and Tasseled Cap Transformation (TCT) have been used to analyze the changes in the vegetation pattern, health and density. Secondary assessment based on surface temperature (derived using thermal infrared bands) have also been attempted. It has been observed that during the years 2006 to 2016, moderate to dense vegetation has decreased drastically due to the intense mining going on in the area. Surface temperature data obtained shows a constant increase during the ten year period apparently due to coal fires. The utility of remote sensing data in such studies has been emphasized.

1. INTRODUCTION

Coal is one of the most abundantly available fossil fuels around the globe which meets a major part of the energy need for human consumption. India is the third largest coal producer in the world after China and USA. For producing more and more coal, mining activities are increasing day-by-day. Although coal mining and related activities provide huge energy resource; however, these adversely affect the environment of the area by digging and causing deforestation.

Jharia coalfield (JCF) has a long history of mining, which started towards the end of the 19th century (Gee, 1940). The mining activities intensified in Jharia in 1920's and thereafter they have been growing extensively and exponentially. JCF is important in the Indian context as it produces largely bituminous coal and is the only coalfield in India that produces coking coal, which is imperative to the steel industry. At present, there are around 35 large underground and opencast mines in the JCF. As a result of mining, environmental changes such as changes in landform, land use/land-cover and vegetation distribution as well as degradation in the quality of air, water, and soil have been occurring since a long time. Besides these, other effects of coal mining include activation of coal fires both surface and subsurface, and subsidence of land surface.

Repetitive multispectral satellite data are available since 1972 onwards. The data have great operational potential for monitoring and surveillance of environmental parameters. This article aims at assessing the impacts caused due to surface coal mining activities by studying the environmental parameters derived using remote sensing data such as normalized difference vegetation index (NDVI), tasseled cap transformation (TCT) and temperature, in a subset of JCF.

2. STUDY AREA

JCF is located in Dhanbad district in the state of Jharkhand, India. The coalfield is a sickle-shaped terrain and covers about 450 sq km area confined between latitude 23° 38' N - 23° 50' N and longitude 86° 07' E - 86° 30' E,

with an average elevation of about 220 m above mean sea level (msl). A small subset has been extracted from the whole image showing mining area in and around Sijua and Angarpathar (area: 4174 hectares) for further detailed processing, analysis and interpretation.

3. DATA USED AND METHODOLOGY

Satellite data of Landsat is the most commonly used data for both vegetation and surface temperature related studies. Multi-temporal Landsat (TM, OLI/TIRS) data ranging from 2006 to 2016 have been used for this study (Table 1). The satellite data have been downloaded from the USGS image catalogue and care has been taken to download the images from nearly the same date to avoid seasonal variation. All the images are geometrically corrected Level 1 products. All the processing has been done using ERDAS Imagine 2010 and ArcGIS 9.3 software.

Table 1. Specifications of Landsat data used in the study

SENSOR	DATE	BANDS USED	SPATIAL RESOLUTION (m)
TM	26 Dec. 2006	Band 3 (Red)	30 (Band 3 and 4)
	21 Dec. 2010	Band 4 (NIR) Band 6 (TIR)	120* (Band 6)
OLI/TIRS	21 Dec. 2016	Band 4 (Red) Band 5 (NIR) Band 10 (TIRS 1)	30 (Band 4 and 5) 100* (Band 10)

*TIR/TIRS bands are acquired at 120/100 m resolutions, but are resampled to 30 m in delivered data product.

3.1 Pre-processing

For Landsat TM data, the digital number (DN) values have been converted to spectral radiance and then into Top of Atmosphere (TOA) reflectance using the formulae given below (Chander et al., 2009):

$$L^* = \frac{(L_{\max} - L_{\min})DN + L_{\min}}{DN_{\max}} \quad (1)$$

$$\rho_g = \frac{\pi L^* d^2}{E_{\text{sun}} \cos \theta_s} \times 100 \quad (2)$$

where L^* = spectral radiance received at the sensor; L_{\min} and L_{\max} are respectively the minimum and the maximum detected spectral radiance for the sensor; DN_{\max} = maximum grey level; DN = digital number for the pixel; ρ_g = reflectance in the band; E_{sun} = mean solar exo-atmospheric spectral irradiance in the band; d = Earth-sun distance (Astronomical units); $\cos \theta_s$ = solar zenith angle (degrees). It can also be described as sine of the solar elevation angle. The L_{\min} , L_{\max} and θ_s values are available in the image metadata file.

Landsat OLI/TIRS datum has been converted to radiance and reflectance using equation (3) and (4) respectively (USGS, 2014):

$$L^* = M_L Q_{\text{cal}} + A_L \quad (3)$$

$$\rho_\lambda = \frac{M_p Q_{\text{cal}} + A_p}{\sin(\theta_s)} \quad (4)$$

where L^* = TOA spectral radiance (Watts/($m^2 * \text{srad} * \mu\text{m}$)); M_L = band-specific multiplicative rescaling factor (RADIANCE_MULT_BAND); A_L = band-specific additive rescaling factor (RADIANCE_ADD_BAND); Q_{cal} = quantized and calibrated standard product pixel values (DN); M_p = band-specific multiplicative rescaling factor (REFLECTANCE_MULT_BAND); A_p = band-specific additive rescaling factor

(REFLECTANCE_ADD_BAND); $\rho\lambda$ = TOA planetary reflectance; θ_s = local sun elevation angle. All this data is available from the metadata file of the images.

3.2 NDVI

NDVI is generally considered as a good indicator of vegetation vigour, density and health in an area. In order to have an estimate of the temporal variation of NDVI over the years, a study has been carried out using Landsat images of 2006, 2010, and 2016. NDVI was first conceived by Rouse et al., (1973) and is calculated as follows:

$$NDVI = \frac{NIR - Red}{NIR + Red} \quad (5)$$

where Red and NIR are the spectral reflectance of vegetation in the red band and the near infrared band respectively. Theoretically, NDVI values range from -1 to +1 where -1 corresponds to water bodies and +1 to very dense vegetation. NDVI images have been generated from nearly the same date to avoid seasonal variation. The images have been density sliced to divide the area into three classes as defined by Gangopadhyay *et al.*, (2006):

- i. **Non-vegetated Area:** Pixels having NDVI values below 0.2. It includes water bodies, barren lands, open pits, exposed overburden dumps, built-up areas, coal processing plants and other such areas having no vegetation.
- ii. **Sparse Vegetation:** Pixels having NDVI values between 0.2 and 0.5. It includes areas covered with shrubs, herbs, small trees etc.
- iii. **Moderate to Dense Vegetation:** Pixels having NDVI values above 0.5. It includes natural forests/dense vegetation, reclaimed and similar areas.

3.2. TCT

In order to derive information about the development and health of vegetation and soil condition in JCF, TCT has been used. It enhances the spectral information of the data. Usually, the first three transformed bands of TCT are used. Band 1 gives the Brightness (measure of soil), band 2 gives Greenness (measure of vegetation) and band 3 gives wetness (interrelationship of soil and canopy moisture). The TC indices are calculated using the equation (6),

$$TC_i = (Co_1 * band1) + (Co_2 * band2) + (Co_3 * band3) + (Co_4 * band4) + (Co_5 * band5) + (Co_6 * band6) \quad (6)$$

where TC_i is the calculated tasseled cap index for Brightness, Greenness, or Wetness depending on the coefficients (Co_i) used. The coefficients for calculation of TCT have been taken from Crist and Cicone, (1984) for TM and Baig *et al.*, (2014) for OLI.

3.3. Temperature

Radiance images derived from thermal bands have been used to calculate at-sensor brightness temperature. Equation (7) has been used to calculate temperature (in Kelvin) for TM and OLI/TIRS images (Chander *et al.*, 2009; USGS, 2014)

$$T_r = \frac{K2}{\ln\left(\frac{K1}{L^*} + 1\right)} \quad (7)$$

where T_r = radiant temperature (K); $K1$ and $K2$ = band specific thermal conversion calibration constants 1 and 2 respectively ($W / (m^2 sr \mu m)$); L^* = spectral radiance; \ln = natural logarithm. The temperature images have been later density sliced keeping the background temperature equal to 25°C.

4. RESULTS AND DISCUSSIONS

4.1 NDVI

Changes in NDVI have been used as a criteria for determining changes in vegetation in Sijua-Angarpathar area (Figure 1). The pie charts (Figure 2) correspond to the areal distributions of the three classes (in percentage) in 2006, 2010 and 2016. Upon comparison, it has been observed that moderate to dense vegetation has decreased from 2006 to 2016 with a corresponding increase in non-vegetated areas, as the mining and related activities proceeded. The reason for this is the direct loss of vegetation when the surface is cleared for initiation of mining activity in an

area or covered under overburden material or there is an increase in settlements around the mines. Apart from this, indirect effects leading to loss of vegetation include a) contamination of soil due to increase in heavy metal content as a result of coal dust, b) loss of photosynthetic activity as the dust forms a layer on the leaf surface, and c) possibly lowering down of water table ultimately leading to drying up and death of the plants. Loss of vegetation has negative impacts on the ecology of the area as the vegetation-free areas become prone to wind and water erosions, as also habitat deterioration and degradation of living conditions for animal species etc.

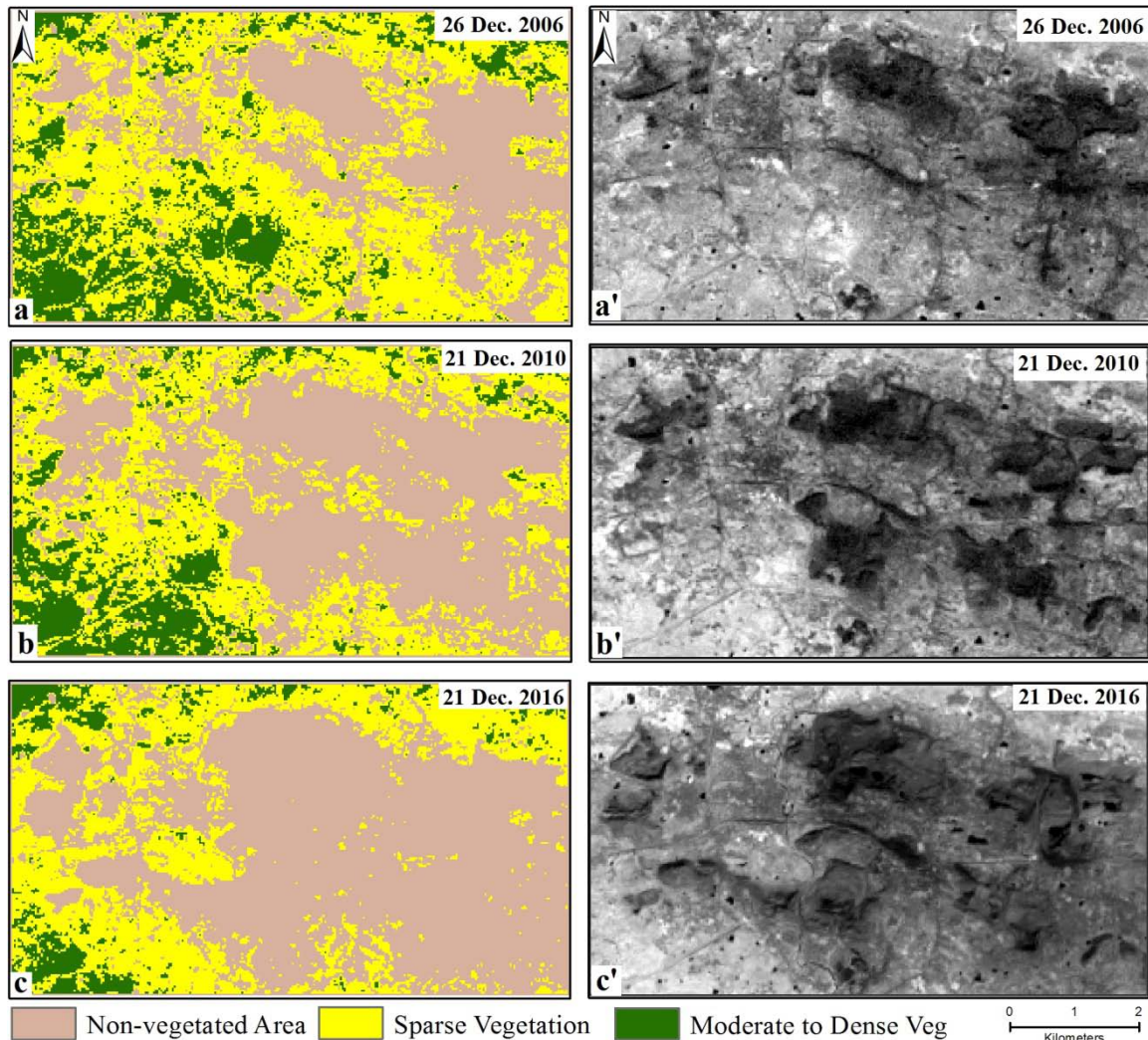


Figure 1. Density sliced NDVI images of Sijua-Angarpathar area are shown in a,b,c, while a', b', c' show the original NDVI images generated from Landsat data of the period 2006 to 2016. The white/lighter areas correspond to the vegetation while black/darker areas correspond to the non-vegetated areas.

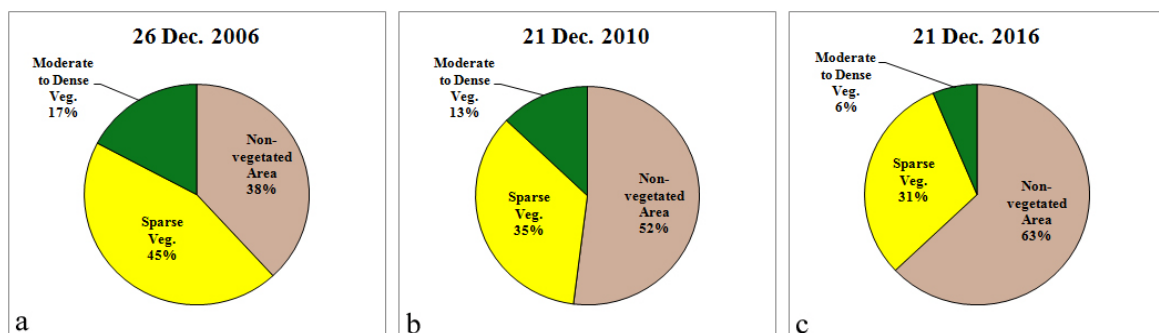


Figure 2. Pie charts showing variation in vegetated and non-vegetated areas of Sijua-Angarpathar (total area 4174 hectares) over the years corresponding to Figure 1 above. Note the decrease in Moderate to Dense vegetation from 17% to 6% over a span of a decade.

4.2 TCT

In order to evaluate the spatial distribution of vegetation condition for different years, the components of tasseled cap have been mapped. The Brightness and Greenness are equivalent to the soil brightness index and the green vegetation index respectively. Brightness image of 2006 has been subtracted from the Brightness image of 2016 to get the difference image (ΔBR). Similarly, difference in Greenness (ΔGR) has been calculated using 2006 and 2016 images. In the Brightness difference image, values above zero means an increase in Brightness and in Greenness difference image, values above zero means a decrease in Greenness (Zhang and Ban, 2010). A colour composite ($R = \Delta BR$; $G = \Delta GR$; $B = \Delta BR$) has been produced to show the areas that have undergone changes (Figure 3). The areas shown in white represent the areas that have increased in Brightness and decreased in Greenness over the 10 year period. The single change in Brightness or Greenness is highlighted in purple or green colours correspondingly. From the studies conducted here, it is observed that the Greenness is high in some regions which has later reduced over the time pointing to the fact that vegetation has decreased in these regions over the years.

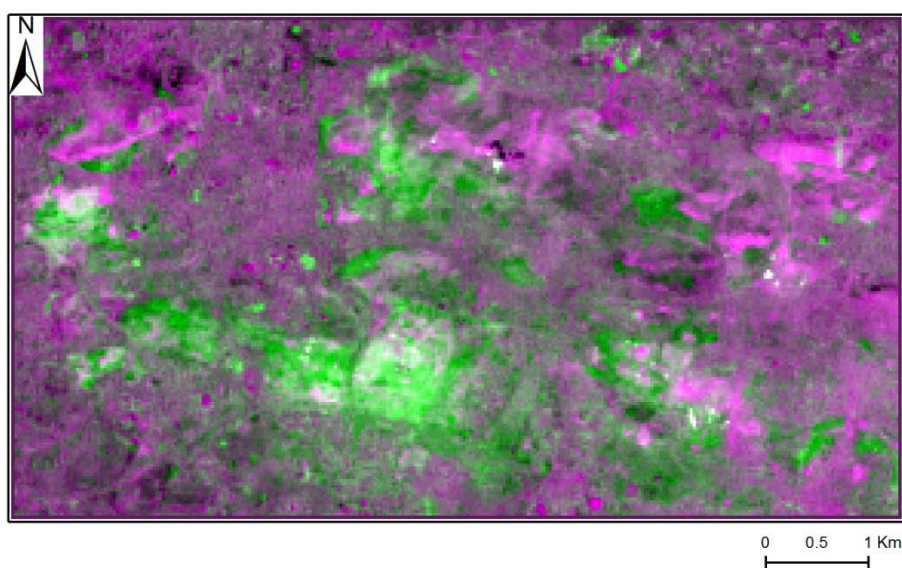


Figure 3. Colour composite ($R = \Delta BR$; $G = \Delta GR$; $B = \Delta BR$) showing the change in Brightness and Greenness from 2006 to 2016.

4.3 Surface Temperature

JCF is infamous for its coal mine fires which have been burning for over a century. Coal fire areas are marked by a sudden rise in ground temperature relative to the background. This rise is very conspicuous when the fire is exposed on the surface, but it is less pronounced in the case of subsurface fires. The objective is to assess the impact of fires on the surface and surrounding areas. Temperature images help to find out the hotspots where there may be a surface or subsurface fire. The temperature images have been density sliced. The threshold temperature has been defined in the context of earlier studies (Martha *et al.*, 2010; Mishra *et al.*, 2011; Gupta *et al.*, 2013). Since December is one of the coldest months in Dhanbad district, therefore the average surface temperature in JCF is assumed to be very less except in the case of fires. For delineating fire areas, the background temperature has been kept as 25°C and fire areas have been shown as those having temperature $>25^{\circ}\text{C}$ (Figure 4). Actual surface temperature has not been taken into consideration as the primary aim here is to qualitatively determine the location and spatial extent of fires. These areas form the 'hotspots'.

Upon analysis, it has been observed that the minimum and maximum temperature in Sijua-Angarpathar area has been increasing since 2006 (Table 2). Further, in 2006 the high temperature areas have covered most of the scene (Figure 4a) but then they start decreasing by 2010 (Figure 4b). Ultimately, by the year 2016, the high temperature areas seem to consolidate in some patches towards the central and eastern side of the scene (Figure 4c). The probable reasons for low temperatures in the western side by 2016 (as compared to 2006) may be that:

- i. there must be a small amount of coal that might have been exhausted due to continuous burning over a period of time;

- ii. the coal present there may have been extracted so that there is no fuel left for the fire; or
- iii. the fire has been controlled due to various reclamation and fire control measures adopted by BCCL.

The high temperature areas corresponding to coal fires cast a serious impact on the environment. Oxides of N and S react with volatile organic compounds (released due to coal fires) in the presence of sunlight to form smog which in turn leads to a number of harmful effects on humans, plants and animals. During rainfall, NO_x and SO_x combine with water droplets and reduce their pH leading to acid rains. Though an exact amount of greenhouse gases released due to fires is not quantified but they play a significant role in global warming. The soil above the fire areas is devoid of moisture and is baked. The soil friendly organisms (bacteria, nematodes, earthworms etc.) die under such harsh conditions, thus limiting the ability of the soil to support vegetation. The existing vegetation also dries up and ultimately dies due to the lack of water and other nutrients.

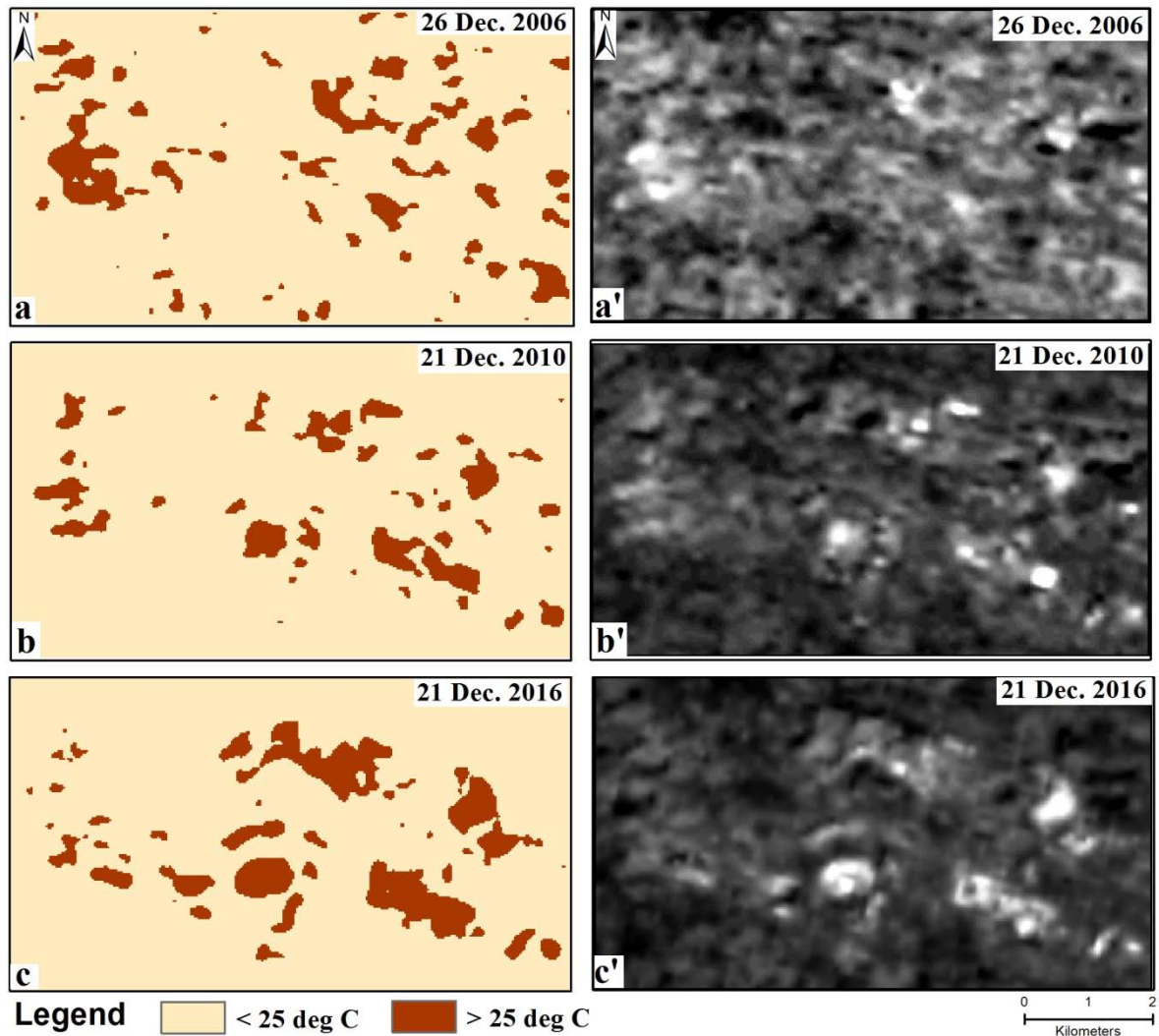


Figure 4. Density sliced surface temperature images derived from Landsat data of the years (a) 2006, (b) 2010, and (c) 2016. The corresponding original surface temperature images have been shown in a',b',c'. The white spots in the otherwise grey background are the high temperature areas which stand out distinctively against the lower background temperature areas.

Table 2: Minimum and maximum temperature over the years

Date	Minimum Temperature (K)	Maximum Temperature (K)
26 Dec. 2006	291.5	304.8
21 Dec. 2010	292.7	308.6
21 Dec. 2016	294.3	310.8

5. CONCLUSION

JCF has a long mining history. Intensive mining activities in the JCF over more than a century have brought out significant environmental changes in the area. The present study concludes that mining has led to a decrease in vegetation in some locations over the ten year period ranging from 2006 to 2016. Also, TCT shows that there has been changes in Brightness and Greenness of the area over the decade long study period. Increase in temperature over the years (2006 to 2016) also points to the fact that apparently the fire is increasing over the years. The findings of this research clearly show the effect of mining on the environment. The study demonstrates that repetitive satellite data (of adequate spatial resolution) hold considerable promise for assessing the impact of surface coal mining on the environment over the years and its monitoring. This may help the planners and managers in developing environmental management strategies on a long term basis.

ACKNOWLEDGEMENT

V. Saini is grateful to the University Grants Commission (UGC), New Delhi, for providing financial assistance in the form of Research Fellowship. The authors thank the USGS (<http://glovis.usgs.gov/>) for providing the Landsat data used in this work free of cost through the internet.

REFERENCES

- [1] Baig, M.H.A., Zhang, L., Shuai, T., Tong, Q., 2014. Derivation of a tasseled cap transformation based on Landsat 8 at-satellite reflectance. *Remote Sensing Letters*, 5(5), pp. 423-431.
- [2] Chander, G., Markham, B.L., Helder, D.L. 2009. Summary of current radiometric calibration coefficients for Landsat MSS, TM, ETM+, and EO-1 ALI sensors. *Remote Sensing of Environment*, 113(5), pp. 893-903.
- [3] Crist, E.P., Cicone, R.C., 1984. A Physically-Based Transformation of Thematic Mapper Data-the TM Tasseled Cap. *IEEE Transactions on Geoscience and Remote Sensing*, GE-22(3), pp. 256-263.
- [4] Gangopadhyay, P.K., Lahiri-Dutt, K., Saha, K. 2006. Application of remote sensing to identify coalfires in the Raniganj coalbelt, India. *International Journal of Applied Earth Observation and Geoinformation*, 8(3), pp. 188-195.
- [5] Gee, R.E., 1940. History of coal mining in India. *Geological Survey of India*, 6, pp. 313-318.
- [6] Gupta, N., Syed, T. H., Athiphro, A., 2013. Monitoring subsurface coal fires in Jharia coalfield using observations of land subsidence from differential interferometric synthetic aperture radar (DInSAR). *Journal of Earth System Science* 122, pp. 1249-1258.
- [7] Martha, T.R., Guha, A., Kumar, K.V., Kamaraju, M.V.V., Raju, E.V.R., 2010. Recent coal-fire and land-use status of Jharia Coalfield, India from satellite data. *International Journal of Remote Sensing*, 31, pp. 3243-3262.
- [8] Mishra, R.K., Bahuguna, P.P., Singh, V.K., 2011. Detection of coal mine fire in Jharia coal field using Landsat-7 ETM+ data. *International Journal of Coal Geology*, 86, pp. 73-78.
- [9] Rouse, J.W., Haas, R.H., Schell, J.A., Deering, D.W., 1973. Monitoring vegetation systems in the Great Plains with ERTS. *Proceedings of 3rd ERTS Symposium*, NASA SP-351 I, pp. 309-317.
- [10] USGS, 2014. Using the USGS Landsat 8 product. Retrieved December 11, 2014 from <https://landsat.usgs.gov/using-usgs-landsat-8-product>.
- [11] Zhang, Q., Ban, Y., 2010. Monitoring impervious surface sprawl using tasseled cap transformation of Landsat data, edited by Wagner, W., Szekely, B., *Proceedings of the 8th ISPRS TC Symposium*, Vol. XXXVIII, pp. 311-315.